Accurate Dynamic Modelling of Hydraulic Servomechanisms

Manuel Pencelli, Renzo Villa, Alfredo Argiolas, Gianni Ferretti, Marta Niccolini,
Matteo Ragaglia, Paolo Rocco and Andrea Maria Zanchettin

***Abstract*—In this paper, the process of modelling and identification of a hydraulic actuator is discussed. In this framework a simple model based on the classical theory has been derived and a first experimental campaign has been performed on a test bench. These tests highlighted the presence of unmodeled phenomena (e.g. dead-zone, hysteresis, etc.), therefore a second and more extensive experimental campaign has been done. With the acquired knowledge an improved model has been developed and its parameters identified. Finally several experimental tests have been performed in order to validate the model.**

***Index Terms*—Hydraulic systems, Hydraulic actuators, Identification**

I. Introduction

Hydraulic actuators are increasingly gaining ground in the development of servomechanism because of their high power density, reliability and relatively low maintenance costs. These features make these actuators particularly fit for several application domains such as earthwork and constructions machinery [1], [2], mining industry [3], forestry and agriculture [5]. However, hydraulic actuators are typically controlled by heavily approximated controllers that cannot guarantee good performance of accuracy and repeatability. In order to develop an accurate and reliable control algorithm, a deep knowledge of the controlled system is usually needed. For this reason, in the last few years the scientific community put a significant effort in studying the behaviour of hydraulic systems. In this regard a general overview of hydrostatic and control-oriented modelling is presented in [6]. Since the valve is a critical component in hydraulic servomechanisms, many studies have been done over the years. For instance, a unified proportional valve model is presented [7], while in [8] a detailed model which also take into account the electro-mechanical dynamics of the valve is discussed. In [9] the authors propose a physical model with a complete description of the flow dynamics behaviour in function of the geometric properties of the system. A simplified control-oriented model for a hydraulic servomechanism is shown in [4]. In the framework of an application concerning robotics a physical analysis of hydraulic actuators is presented in [10]. For the sake of completeness it is also necessary to highlight the existence of alternative approaches. For instance, in [11] a black box modeling of a hydraulic drive based on neural networks is shown, while in [12] a similar problem is solved using a weighted least squares approach. Finally in [13] electro-hydraulic actuator is modeled by using Adaptive Neuro-Fuzzy Inference System. That said, in order to have a clear understanding of the physical phenomema affecting the various components, machine learning methods along with other black box modeling techniques have not been considered in this work. The aim of this paper is to analyze the main phenomena characterizing the behaviour of hydraulic actuators and propose a practical identification procedure in order to develop an accurate mathematical model. Specifically, simple models for the components of the system (piston, valve and load) are developed according to the classical literature. Then, the results of the first experimental campaign pointed out that some unmodeled phenomena, such as the valve dead-zone and internal leakage, were inducing high inaccuracies. Therefore a second experimental campaign has been conducted in order to investigate in detail the behaviour of the system and an improved model has been derived according to the gathered knowledge. Finally, after the selection of specific performance index, several tests have been performed in order to validate the model. The remainder of this paper is organized as follows. Section II describes the experimental set up and presents the first simple model of the servomechanism. In Section III the first experimental campaign is briefly described and some unmodeled phenomena are pointed out. Then, in Section IV, the improved models for the components of the system are discussed, together with a new and more extensive experimental campaign. The validation of the overall model is showed in Section V. Finally, conclusions and future developments are presented in Section VI.

Manuel Pencelli (manuel_pencelli@yanmar.com), Alfredo Argiolas, Marta Niccolini and Matteo Ragaglia are with Yanmar R&D Europe, Viale Galileo, 3 - 50125 Firenze, Italy.

Manuel Pencelli, Renzo Villa, Gianni Ferretti, Paolo Rocco and Andrea Maria Zanchettin are with Politecnico di Milano, Dipartimento di Elettronica, Informazione e Bioingegneria, Piazza L. Da Vinci 32, 20133, Milano, Italy.

II. Hydraulic Servomechanism Model

The hydraulic servomechanism that will be analyzed in this paper is shown in Figure 1. The system is composed by two separated hydraulic servomechanism. Each piston rod is rigidly connected to the load mass, that consists in a plate constrained by vertical motion guides on top of which it is possible to load a weight. The oil flow rate is determined by two 3/4 directional valves. The entire system is powered by an hydraulic pump, equipped with a safety release valve. The test bench is also equipped with the following sensors: 2 linear potentiometers that measure the position of each cylinder, 5 pressure sensors installed at the outlet of the pump and inside the four chambers of the two cylinders, and 2 load cells installed between the rod side of each cylinder and the plate.

At first, a preliminary dynamical model was obtained from classical hydraulic equations. The hydraulic piston is described by (1), the valve characteristic is given by (2) and (3), and the mechanical equation by (5):

978-3-9819263-2-3/DATE19/©2019 EDAA

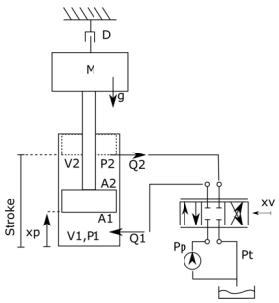

Fig. 1: Hydraulic system with compressive load.

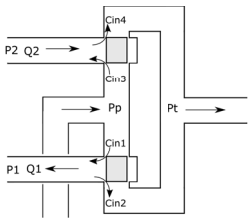

Fig. 2: Valve scheme with internal leakages.

$$\dot{P}_1 = \frac{\beta(Q_1 - A_1\dot{x}_p)}{V_1(x_p)}, \quad \dot{P}_2 = \frac{\beta(-Q_2 + A_2\dot{x}_p)}{V_2(x_p)} \tag{1}$$

$$Q_1 = sign(x_v)\frac{\pi}{4}\frac{d^2 x_v^2}{\sqrt{1-x_v^4}}\sqrt{\frac{2}{\rho}\Delta P_1} \tag{2}$$

$$Q_2 = sign(x_v)\frac{\pi}{4}\frac{d^2 x_v^2}{\sqrt{1-x_v^4}}\sqrt{\frac{2}{\rho}\Delta P_2} \tag{3}$$

$$\Delta P_1 = \begin{cases} P_p - P_1, \ x_v \geq 0 \\ P_1 - P_t, \ x_v < 0 \end{cases} \quad \Delta P_2 = \begin{cases} P_2 - P_t, \ x_v \geq 0 \\ P_p - P_2, \ x_v < 0 \end{cases} \tag{4}$$

$$\ddot{x}_p = \frac{1}{M}(A_1 P_1 - A_2 P_2 - D\dot{x}_p - Mg) \tag{5}$$

where P_1 (P_2), V_1 (V_2), Q_1 (Q_2), A_1 (A_2) are, respectively, the bottom-side (rod-side) chamber pressure, chamber volume, flow rate and surface area. , P_p is the pump side pressure, P_t is the tank pressure, x_p is the piston position, β is the mineral oil bulk modulus, x_v is the valve control signal, d is the nominal orifice diameter, and ρ is the mineral oil density. M is the load mass, D is the viscous friction coefficient and g is the gravitational acceleration. Combining equations (1) and (5) the following formulation is obtained:

$$\begin{cases} \frac{d}{dt}x_p = \dot{x}_p \\ \ddot{x}_p = \frac{1}{M}[A_1 P_1 - A_2 P_2 - D\dot{x}_p - Mg] \\ \dot{P}_1 = \frac{\beta}{V_1(x_p)}(Q_1 - A_1\dot{x}_p) \\ \dot{P}_2 = \frac{\beta}{V_2(x_p)}(-Q_2 + A_2\dot{x}_p) \end{cases} \tag{6}$$

where Q_1 e Q_2 are defined by (2) and (3). Equation (6) is a 4th order non linear system with state variables $x_p, \dot{x}_p, P_1, P_2$ and control variable x_v.

III. First Experimental Campaign

The results of the first experimental campaign shown some discrepancies between the measured data and the previous model. Figure 3 shows the system response to a trapezoid valve opening signal. The pressures drop quickly when the valve is closing, thus indicating the presence of some leakages inside the valve. Furthermore, the distance covered by the piston is not equal for the two directions of the valve opening. This asymmetry can be determined by either a different pressure drop or an asymmetric valve characteristic.

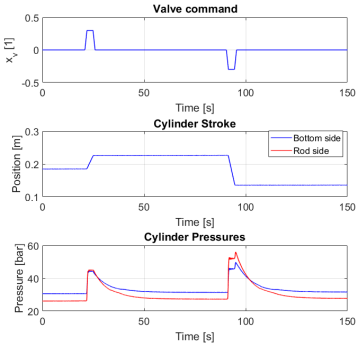

Fig. 3: Experimental result, trapezoid signal with amplitude ± 0.3 and rising time $1s$.

IV. Dynamic Model Refinement

In order to model all the newly observed phenomena and identify the dynamic parameters, many tests have been performed, and a steady state analysis has been done. Trapezoidal signals were preferred as inputs with respect to step signals, avoiding to excessively stress the system. In the remainder of this Section the most significant phenomena and the corresponding identification procedures will be discussed.

A. Interpolant polynomials

To efficiently represent the system's asymmetry observed in Section III, proper corrective terms were introduced to the valve characteristic equations:

$$Q_1 = \begin{cases} k_1^+ \alpha\sqrt{\frac{2}{\rho}(P_p - P_1)}, & x_v \geq 0 \\ k_1^- \alpha\sqrt{\frac{2}{\rho}(P_1 - P_t)}, & x_v < 0 \end{cases} \tag{7}$$

$$Q_2 = \begin{cases} k_2^+ \alpha\sqrt{\frac{2}{\rho}(P_2 - P_t)}, & x_v \geq 0 \\ k_2^- \alpha\sqrt{\frac{2}{\rho}(P_p - P_2)}, & x_v < 0 \end{cases} \tag{8}$$

where:

$$\alpha = sign(x_v)\frac{0.25\pi(dx_v)^2}{\sqrt{1-x_v^4}} \tag{9}$$

In order to identify the new parameters, the valve has been fed with several trapezoid PWM signals, and the system steady-state has been analyzed for a total of 30 experiments. The identification procedure has been performed by assuming a constant applied load and by taking the middle position of the piston: $\bar{x}_p = (x_p^{MAX} - x_p^{min})/2$ as working point. In this way it was possible to consider null the pressures derivative, given a steady-state velocity:

$$\frac{\beta\ (Q_1 - A_1\dot{x}_p)}{V_1(\bar{x}_p)} = \frac{\beta\ (-Q_2 + A_2\dot{x}_p)}{V_2(\bar{x}_p)} = 0 \tag{10}$$

Consequently, by substituting (7), (8) and (9) in (10), the parameters $k_i^{-/+}$, $i = 1, 2$ are obtained as follows:

$$k_i^{-/+} = \frac{A_i\dot{x}_p}{\sqrt{\frac{2}{\rho}(\Delta P_i)}}\frac{\sqrt{1-x_v^4}}{0.25\pi(dx_v)^2} \tag{11}$$

The trapezoid control signal was characterized by a rising time and falling time of $0.5s$. The amplitude of the trapezoid belongs to the following set: $x_v \in [-1, -0.25] \cup [0.25, 1]$, and every experiment has been performed by incrementing the absolute value of the amplitude by 0.05. Figure 4 shows the results of the identification. The corrective coefficients have been expressed as a function of the control signal x_v, by using proper interpolating polynomials, in order to efficiently model the complex geometry of the spool and its positioning mechanism. For these polynomials the pressure drop has not been taken into account, since the turbolent flow, occourring inside the valve, is already modeled by equations (2) and (3).

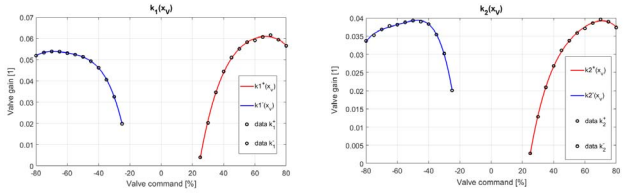

Fig. 4: Iterpolating polynomials.

B. Valve Deadzone and hysteresis

Typically hydraulic valves are characterized by high non-linearities such as hysteresis and dead-zones due to their complex mechanical structure, that has not been considered in the first model. In order to observe and analyze these phenomena, a test with a sinusoidal control signal has been performed. In our case a very accurate evaluation of these phenomena was not possible due to the absence of dedicated sensors. Nevertheless, a reasonable estimation has been done, by neglecting the compressibility of the hydraulic oil and by computing the flow directly from the piston's speed. Figure 5 shows the results of the flow normalized respect to the term $\sqrt{\Delta P_i}$. The overall amplitude of the dead-zones is $dz^- \in [-0.24, -0.17]$ for negative values of the control signal and $dz^+ \in [0.21, 0.28]$ for positive values of the control signal. Furthermore, the hysteresis involves a very small area (close to the dead-zones) of the $q_i/\sqrt{\Delta P_i}$ curve. For this reason, only an average value of the dead-zone has been included in the equations.

C. Valve's flow losses

It is possible to study the internal leakage of the valve when it is closed. Specifically, assuming laminar flow, a set of linear equations can be used:

$$q_1 = C_1(P_p - P_1) - C_2(P_1 - P_t) \tag{12}$$
$$q_2 = C_4(P_2 - P_t) - C_3(P_p - P_2) \tag{13}$$

where C_1, C_2, C_3 and C_4 are the leakage flow coefficients of the valve. Figure 2 shows the overall valve schematic. When the valve is closed the position of the piston can be considered constant, therefore the following decoupled first order linear equations are obtained:

$$\dot{P}_1 = \frac{\beta(-C_2P_1 + C_1P_p)}{V_1},\ \dot{P}_2 = \frac{\beta(-C_4P_2 + C_3P_p)}{V_2} \tag{14}$$

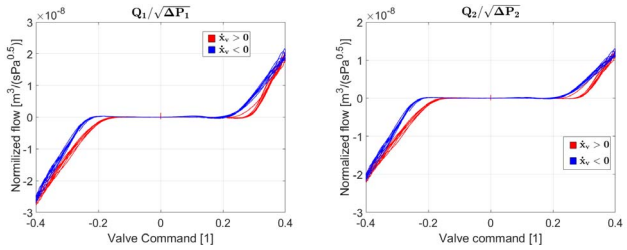

Fig. 5: Valve characteristic curves, normalized respect to square root pressure drop.

thus the transfer functions between the two chamber pressures and the supply pressure P_p is given by:

$$\frac{P_1(s)}{P_p(s)} = \frac{C_1\beta/V_1}{s + \frac{\beta}{V_1}C_2},\ \frac{P_2(s)}{P_p(s)} = \frac{C_3\beta/V_2}{s + \frac{\beta}{V_2}C_4} \tag{15}$$

The coefficients are then identified by analyzing the time constants and the static gains of the pressures transients, using the same experiments discussed in Subsection IV-A. The leakage coefficients shown a strong dependence on the mechanical tolerance and on the rest position of the valve spool, namely hysteresis. For this reason, since a linear model has been chosen, in the equations of the leakage flows only the average values of C_1, C_2, C_3 and C_4 have been used.

D. Mechanichal losses

From the set of trapezoidal tests, the mechanical losses were identified by using data provided by the load cell. When the piston moves at constant speed the mechanical equation is given by:

$$f_{loss}(\dot{x}_p) = A_1P_1 - A_2P_2 - L_{cell} \tag{16}$$

where L_{cell} is the measured force. Figure 6 shows the mechanical losses with respect to the piston speed, computed for each trapezoidal experiment. A Coulombian static friction term generates a discontinuity in the origin. The losses show a quadratic behaviour with respect to the piston speed. This fact indicates the presence of pressure losses, generated by the friction of the fluid inside the hoses. The detailed mechanical balance is obtained by modifying the equation (5):

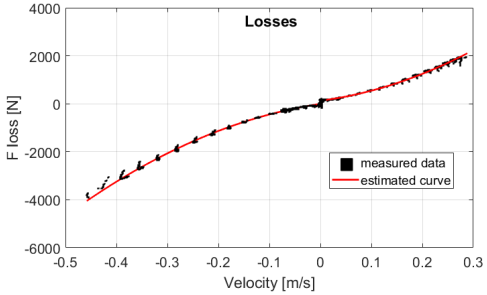

Fig. 6: Mechanical losses as a function of $\dot{x}_p$.

$$\ddot{x}_p = \frac{1}{M}[A_1(P_1 - \Delta P_{1loss}) - A_2(P_2 - \Delta P_{2loss}) + - f_r(\dot{x}_p) - D\dot{x}_p - Mg] \quad (17)$$

where ΔP_{iloss} is the i-th pressure drop due to the previously mentioned friction in the pipeline and $f_r(\dot{x}_p)$ is the Coulombian friction term. Considering negligible the fluid compressibility, gathering all the terms proportional to $\dot{x}_p^2$ together, and given $\zeta = \theta_1 A_1^2 - \theta_2 A_2^2$, the mechanical equation can be rewritten as:

$$\ddot{x}_p = \frac{1}{M}[A_1 P_1 - A_2 P_2 - f_r(\dot{x}_p) - D\dot{x}_p - \zeta \dot{x}_p^2 - Mg] \quad (18)$$

E. Final Model

Finally the overall model that includes the improved hydraulic and mechanical dynamics can be expressed as:

$$\begin{cases} \dot{x}_p = \dot{x}_p \\ \ddot{x}_p = \frac{1}{M}[A_1 P_1 - A_2 P_2 - f_r(\dot{x}_p) - D\dot{x}_p - \zeta \dot{x}_p^2 - Mg] \\ \dot{P}_1 = \frac{\beta}{V_1(x_p)}(Q_1 - A_1 \dot{x}_p) \\ \dot{P}_2 = \frac{\beta}{V_1(x_p)}(-Q_2 + A_2 \dot{x}_p) \end{cases} \quad (19)$$

$$Q_1 = \begin{cases} c_1(P_p - P_1) - c_2(P_1 - P_t) & d_z^- < x_v < d_z^+ \\ k_1^+(x_v)\frac{\pi}{4}\frac{d^2 x_v^2}{\sqrt{1-x_v^4}}\sqrt{\frac{2}{\rho}(Pp - P_1)} & x_v \geq d_z^+ \\ -k_1^-(x_v)\frac{\pi}{4}\frac{d^2 x_v^2}{\sqrt{1-x_v^4}}\sqrt{\frac{2}{\rho}(P1 - P_t)} & x_v < d_z^- \end{cases} \quad (20)$$

$$Q_2 = \begin{cases} c_3(P_p - P_2) - c_4(P_2 - P_t) & d_z^- < x_v < d_z^+ \\ k_2^+(x_v)\frac{\pi}{4}\frac{d^2 x_v^2}{\sqrt{1-x_v^4}}\sqrt{\frac{2}{\rho}(Pp - P_2)} & x_v \geq d_z^+ \\ -k_2^-(x_v)\frac{\pi}{4}\frac{d^2 x_v^2}{\sqrt{1-x_v^4}}\sqrt{\frac{2}{\rho}(P_2 - P_t)} & x_v < d_z^- \end{cases} \quad (21)$$

V. Model Validation

The validation of the model was performed by feeding the valve with several sinusoidal control signals of amplitude $B \in [0.27, 0.35, 0.50]$ and frequency $f = 0.3Hz$ and comparing the experimental data with the simulated ones.

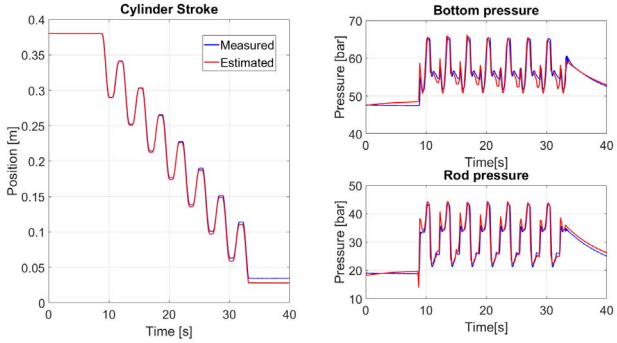

Fig. 7: Validation results, $B = 0.50$

Figures 7 show the validation results in the case of $B = 0.5$. For every simulation the normalized mean squared error was chosen as a performance index. By applying this criterion to the above experiments and simulation the following results are obtained:

TABLE I: NMSE value for the validation tests

Test	$NMSE\|_{x_p}$	$NMSE\|_{\dot{x}_p}$	$NMSE\|_{P_1}$	$NMSE\|_{P_2}$
$B = 0.27$	0.0092	0.0559	0.2052	0.2973
$B = 0.35$	0.0011	0.0104	0.1407	0.1788
$B = 0.5$	0.0005817	0.0016	0.144	0.1093

A good matching of the state variables is achieved. Slightly worse results are observed for $B = 0.27$, in this case the amplitude of the signal is near the valve's deadzone and the hysteresys plays a major role.

VI. Conclusions and Future Developments

In this paper we have analyzed the mathematical model and the main problems affecting servohydraulic mechanism. Proper identification procedure was proposed in order to identify all the dynamic parameters and obtain an accurate model. Even more accurate results can be obtained by using in addition flow sensors and speed sensors.

References

[1] M. Hutter, P. Leemann, S. Stevsic, A. Michel, D. Jud, M. Hoepflinger, R. Siegwart, R. Figi, C. Caduff, M. Loher, and S. Tagmann, "Towards optimal force distribution for walking excavators," in *Advanced Robotics (ICAR), 2015 International Conference on*, July 2015, pp. 295–301.

[2] M. Tanzini, J. M. Jacinto-Villegas, A. Filippeschi, M. Niccolini, and M. Ragaglia, "New nteraction metaphors to control a hydraulic working machine's arm," in *IEEE Symposium of Safety and rescue Robotics (SSRR)*, 2016.

[3] P. Corke, J. Roberts, J. Cunningham, and D. Hainsworth, *Mining Robotics*. Berlin, Heidelberg: Springer Berlin Heidelberg, 2008, pp. 1127–1150. [Online]. Available: https://doi.org/10.1007/978-3-540-30301-5_50

[4] W. Li and G. Tao, "Modeling cylinder controlled by servo valve of hydraulic looper in hot strip mill," in *Chinese Automation Congress (CAC), 2015*. IEEE, 2015, pp. 102–107.

[5] J. Billingsley, A. Visala, and M. Dunn, *Robotics in Agriculture and Forestry*. Berlin, Heidelberg: Springer Berlin Heidelberg, 2008, pp. 1065–1077.

[6] N. Manring, *Hydraulic control systems*. Wiley New York, 2005.

[7] B. Eryilmaz and B. H. Wilson, "Unified modeling and analysis of a proportional valve," *Journal of the Franklin Institute*, vol. 343, no. 1, pp. 48–68, 2006.

[8] S. Voronin, E. Maklakova, V. Gasiyarov, and A. Maklakov, "The simple hydraulic drive model of the typical industrial mechatronic system," in *Industrial Engineering, Applications and Manufacturing (ICIEAM), International Conference on*. IEEE, 2016, pp. 1–5.

[9] J. J. Janković, N. B. Petrović, and Č. B. Mitrović, "Control system modeling of hydraulic actuator with compressible fluid flow," *FME Transactions*, vol. 40, no. 2, pp. 75–80, 2012.

[10] Y. Efe, "Dynamic model of a hydraulic servo system for a manipulator robot," 2014.

[11] O. Carsten, "Modeling a hydraulic drive using neural networks," 2001.

[12] E. Guillo, M. Gautier, F. Louveau, and C. Bidard, "Dynamic modelling and identification of a hydraulic servoactuator," *IFAC Proceedings Volumes*, vol. 30, no. 20, pp. 119–124, 1997.

[13] T. G. Ling, M. F. Rahmat, and A. R. Husain, "Anfis modeling of electro-hydraulic actuator system through physical modeling and fcm gap statistic in initial fis determination," *Journal of Intelligent & Fuzzy Systems*, vol. 27, no. 4, pp. 1743–1755, 2014.

[14] N. Ishak, M. Tajjudin, H. Ismail, and R. Adnan, "System identification and model validation of electro-hydraulic actuator for quarter car system," 2006.